

Fan-out intensity optimization of bidirectional photopolymer hologram-based optical backplane bus

Chunhe Zhao

Ray T. Chen, MEMBER SPIE

University of Texas at Austin

Department of Electrical and Computer Engineering

Austin, Texas 78758

E-mail: raychen@uts.cc.utexas.edu

Abstract. Fabrication of the bidirectional optical backplane bus, employing arrays of multiplexed polymer-based waveguide holograms on a waveguiding plate, is reviewed. An analysis of its functionality is presented for the first time. After an objective function for the system is established, the fan-out intensity fluctuations among all the different channels are minimized by solving a set of nonlinear equations numerically. To further ensure the validity of our calculation, a different objective function is considered and the same optimized result is obtained. Particularly, we optimized the fan-out distribution for the case in which nine boards on one side of the optical bus are presented. It was found that a globally optimized diffraction efficiency distribution exists and the minimum fan-out intensity after optimization is about 1.5% of the incident power, which means a minimum laser diode power for this bidirectional optical bus has to be above 7.0 mW for a system speed of 1.2 Gbit/s and a bit error rate of 10^{-15} . Finally, the surface normal fanout beams come out of both directions of the backplane. Therefore, the best hardware implementation scheme integrates the processor/memory boards on both sides of the backplane bus. As a result, the optimal number of processor/memory boards is 16, i.e., $9 + (9 - 2)$, rather than 9. © 1996 Society of Photo-Optical Instrumentation Engineers.

Subject terms: optical backplane bus; diffraction efficiency; optimization; volume holograms.

Paper 18045 received Apr. 22, 1995; revised manuscript received Sep. 18, 1995; accepted for publication Sep. 25, 1995. This paper is a revision of a paper presented at the SPIE conference on Optoelectronic Interconnects III, Feb. 1995, San Jose, CA. The paper presented there appears (unrefereed) in SPIE Proceedings Vol. 2400.

1 Introduction

Currently, most computer backplane buses are electrically interconnected. Due to the increase of clock speed and data transfer rate, electrical interconnection imposes many limitations on high performance computers. These include wide interconnection time bandwidths, large clock skew and large resistance-capacitance (RC) and resistance-inductance-capacitance (RLC) time constraints.¹ Contrary to electrical interconnection, optical interconnection has drawn significant interest²⁻⁴ due to its high data transfer rate, large fan-out densities, and the elimination of capacitive and inductive loading effects. Recently we presented a bidirectional optical backplane bus for a high performance system containing nine processor/memory boards, operating at 632.8 and 1300 nm.⁵ This backplane bus employs arrays of polymer-based multiplexed holograms in conjunction with a waveguiding plate within which bidirectional substrate guided waves are generated. For a single bus line, we demonstrated a data transfer rate of 1.2 Gbit/s at 1.3 μm wavelength. The cascaded characteristic of the fan-out beams away from the incident channel was also demonstrated.

For the cascaded fan-out system reported in Ref. 5, its performance is always limited by the output channel with

the lowest fanout intensity within the 72 (9×8) interconnects. Accurately analyzing this limitation is one of the major concerns in designing a many-to-many cascaded fanout system. In this paper, we theoretically embark on this problem by minimizing the fluctuations among all the output channels so that the intensities of all the fan-out beams are closest to their average value. To fully understand the working mechanism of the bidirectional optical bus, a theoretical analysis for the holographic grating diffraction is carried out first. An objective function for the system aimed at providing an optimized result is further established together with a set of nonlinear equations as functions of the diffraction efficiencies of all the channels. To demonstrate the validity of our calculations, we also developed a separate objective function. The same optimized result is obtained. Finally, theoretical results equivalent to the experimentally demonstrated system previously reported⁵ are presented, and limitations imposed on the system design and performance based on the optimization results are addressed.

2 Architecture of the Bidirectional Optical Backplane Bus

Figure 1 is the schematic of how the developed optical bus can be used as a backplane in multiprocessor, high perfor-

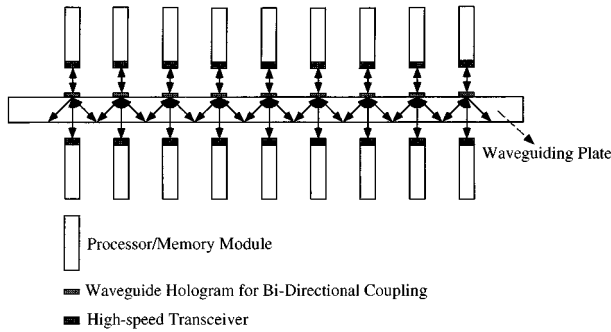


Fig. 1 Schematic depicting the functionality of the bidirectional optical backplane bus in a multitransceiver system containing the demonstrated multiplexed waveguide hologram arrays in conjunction with a waveguiding plate.

mance optoelectronic computers. Bidirectional signal flows are illustrated between the backplane and the processor/memory boards, where the multichip modules (MCMs) are located. With the design that we employed, the optical backplane can serve the purpose of a bidirectional bus. Multiplexed holograms are employed to facilitate two-way communications among boards that are connected to the backplane.

The physical layer of the optical backplane bus is essentially a thin waveguiding plate with a multiplexed hologram array integrated on its surface.⁵ The substrate serves as the light-guiding medium. Both dichromated gelatin⁶ (DCG) and Dupont photopolymer were used as the hologram recording medium. Two hologram arrays were fabricated on the substrate to provide the required bidirectional surface-normal coupling, as indicated in Fig. 1. Both arrays are volume holograms. By definition, a volume holographic grating is described as a grating that produces Bragg diffraction and exhibits strong angular and wavelength selectivity.⁷ For a light beam with a wave vector \mathbf{k} incident on a grating with grating vector \mathbf{K} , a phase-matching condition occurs if

$$\mathbf{k}' = \mathbf{k} - \mathbf{K}, \tag{1}$$

where \mathbf{k}' is the wavevector of the diffracted beam.

Light propagation in the optical backplane bus is actually a combination of consecutive diffraction and reflection processes. After having recorded the two sets of hologram arrays, two grating vectors, \mathbf{K}_1 and \mathbf{K}_2 , are formed in the film [see Fig. 2(a)]. A surface-normal light beam with wavevector \mathbf{k} is incident onto the surface of the film. The two Bragg diffraction conditions occur if

$$\mathbf{k}'_1 = \mathbf{k} - \mathbf{K}_1, \tag{2}$$

$$\mathbf{k}'_2 = \mathbf{k} - \mathbf{K}_2, \tag{3}$$

where \mathbf{k}'_1 and \mathbf{k}'_2 are two diffracted beams generated by the two sets of holographic gratings. The incident light beam is then converted into two substrate modes, i.e., substrate guided waves in this case, propagating along two opposite directions [Fig. 2(b)].

When the substrate guided wave interacts with the gratings on the upper surface as shown in Fig. 2(c), it will be

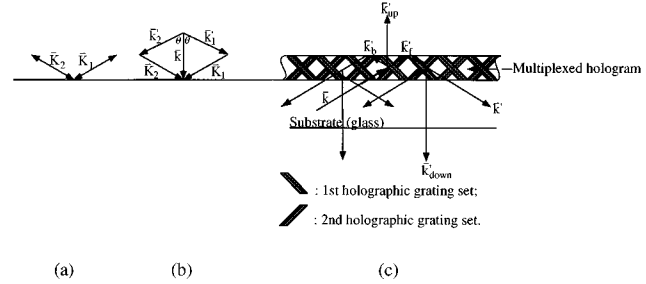


Fig. 2 Diffraction mechanism of light by two sets of hologram gratings recorded on a glass substrate: (a) two grating vectors recorded; (b) light diffraction geometry by the gratings; and (c) light transmission, diffraction and reflection inside the bidirectional backplane bus.

diffracted into three beams due to the cross-coupling effect of the multiplexed hologram.⁸ As a result, a portion of the light beam will be diffracted out of the substrate, giving rise to a surface-normal fan-out \mathbf{k}'_{up} [Fig. 2(c)]. Another portion will be cross-coupled into the beam \mathbf{k}'_b as shown in the figure. The rest of the beam continues to propagate along the original direction, which is indicated as the beam \mathbf{k}'_f in Fig. 2(c). Similarly, after being totally internally reflected (TIR) by the interface between the polymer film and the air, the beams \mathbf{k}'_b and \mathbf{k}'_f will again be, respectively, cross-coupled into three beams as indicated in Fig. 2(c). Note that \mathbf{k}'_{down} is the downward surface-normal fan-out and \mathbf{k}' continues to propagate to the next hologram. Other diffracted beams after the second cross-coupling, due to their back-propagation feature, are unwanted and thus are suppressed by deliberately selecting the objective function in our calculation below. The zig-zag substrate guided waves go through many iterations of this cascaded fan-out process until they hit the last holographic element along the optical path.

From the analysis, the bidirectionality of the optical backplane bus is obvious. Based on the nature of cascaded broadcasting, an inevitable consequence occurs, i.e., the fan-out intensity has a fluctuated distribution away from the incident channel. The major goal of this paper is to minimize the power fluctuation among the experimentally demonstrated 240 (16×15) interconnects containing 16 processor/memory boards on both sides of the optical backplane (Fig. 1).

3 Optimization Process

As the bidirectional substrate guided waves propagate, their intensities will be decreased after each fan-out.⁵ The intensity of each surface-normal fan-out beam is determined by the diffraction efficiency of the corresponding multiplexed holographic gratings. [The diffraction efficiency of a grating in a multiplexed hologram (or sequentially stored gratings in transmission volume holograms) is defined here as the ratio between the power of light diffracted by the grating and that of the incident light when Bragg condition is met. Under this definition, the sum of the diffraction efficiencies of the gratings in a multiplexed hologram should be⁹ less than or equal to 1.] By changing the diffraction efficiency distribution of the holographic grating arrays, we can precisely manipulate the fan-out intensity distribution.

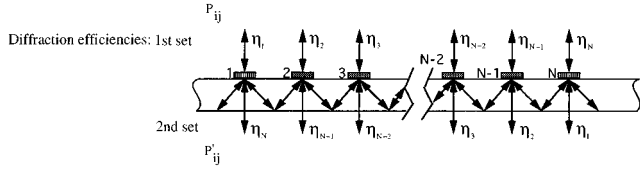


Fig. 3 Schematic of the bidirectional backplane optical bus with N boards on one side of the substrate.

Due to the bidirectionality of the optical bus, it is not feasible for our case to get a uniform fan-out intensity distribution for all the cases where modulated optical signals are incident from different channels. For example, using our architecture, a multiprocessor system containing n processor/memory boards requires $n(n-1)$ interconnects for each bus line to fulfill the broadcasting nature of the backplane bus protocols. Each board needs to be interconnected with the other $n-1$ boards. A uniform fan-out intensity with the first board as the input and the rest as receiving ports will make the power budget the worst when treating the n 'th board as the input and all the other ones as the outputs. In other words, an optimal design shall provide us with a minimized power fluctuation rather than an equalized power distribution among $n(n-1)$ interconnect scenarios.

Figure 3 also shows the schematic of the bidirectional optical bus with N boards on one side of the substrate. To provide the bidirectionality, two arrays of holograms are recorded. In this figure we assume that the diffraction efficiencies of the first set of hologram array are, from left to right, $\eta_1, \eta_2, \dots, \eta_N$, respectively. Due to the symmetric requirement for optimization, the diffraction efficiencies for the second hologram array are $\eta_1, \eta_2, \dots, \eta_N$ from right to left. To provide the optimized power budget, we have to impose the following criteria: $\eta_1=1$ and $\eta_N=0$ for both sets (Fig. 3), i.e., there is only a single set of gratings at the first and the N 'th channels [$\eta_N(\eta_N=0)$] associated, and the second set serves as the input coupler to $N+1, N+2, \dots$ modules which do not exist. If we denote P_{ij} to be the output power at the j 'th channel when the optical signal is incident from the i 'th channel, then the same holds for P'_{ij} , except that they have a reversed fan-out direction (Fig. 3), which has not been employed in the previous demonstration.⁵ Note that the bidirectional hologram arrays provide surface normal fan-out in both directions. Based on these notations, we have

$$P_{ij}=0 \quad \text{whenever } i=j, \quad (4)$$

$$P'_{i1}=P'_{iN}=0 \quad i=1, \dots, N. \quad (5)$$

Furthermore, the nature of fan-out symmetry of the backplane bus also suggests that we can consider only the cases in which the light signal beams are incident from the i 'th channel, with $i=1, \dots, M$ [$M=N/2$ when N is an even number, and $M=(N+1)/2$ when N is an odd number].

To simplify our analysis, we define a transmission function as the energy of a substrate guided light beam transmitted from one hologram to the next. According to the

analysis mentioned above, for a digital optical signal incident from channel 1, the general form of the transmission function can be written as

$$T_{ij}=(1-\eta_{j+1})(1-\eta_{N-j})T_{ij+1} \\ (i=3, \dots, M; j=1, \dots, i-2),$$

$$T_{ii-1}=\eta_{N+1-i} \quad (i=2, \dots, M),$$

$$T_{ii}=0 \quad (i=1, \dots, M), \quad (6)$$

$$T_{ii+1}=\eta_i \quad (i=1, \dots, M),$$

$$T_{ij}=(1-\eta_{j-1})(1-\eta_{N+2-j})T_{ij-1} \\ (i=1, \dots, M; j=i+2, \dots, N),$$

where T_{ij} ($i=1, \dots, M; j=1, \dots, N$) is the energy of light beam transmitted onto grating j when the optical signal is incident from the i 'th channel (see Fig. 3).

In deriving Eq. (6), we treat the input power as 1 and eliminate the Fresnel reflection, which can be easily achieved by an antireflection coating. Accordingly, the general expressions for P_{ij} and P'_{ij} , with $i=1, \dots, M$ and $j=1, \dots, N$, can be represented as

$$P_{ij}=\eta_j(1-\eta_{N+1-j})T_{ij} \quad (i=2, \dots, M; j=1, \dots, i-1),$$

$$P_{ij}=(1-\eta_j)\eta_{N+1-j}T_{ij} \quad (i=1, \dots, M; j=i+1, \dots, N);$$

$$P'_{ij}=(1-\eta_j)^2\eta_{N+1-j}T_{ij} \quad (i=2, \dots, M; j=1, \dots, i-1),$$

$$P'_{ii}=1-\eta_i-\eta_{N+1-i} \quad (i=1, \dots, M), \quad (7)$$

$$P'_{ij}=\eta_j(1-\eta_{N+1-j})^2T_{ij} \quad (i=1, \dots, M; j=i+1, \dots, N). \quad (8)$$

After having been incident onto the i 'th channel of the optical bus, a light beam is diffracted into the glass substrate and propagates to both ends of the backplane bus. Also, the cascaded feature of the outputs (i.e., P_{ij} 's and P'_{ij} 's) from the input channel to the two surface-normal directions of the bus are clearly shown in the preceding expressions.

The description of power budget optimization process now follows. The goal is to find an optimized distribution of diffraction efficiencies leading to a fan-out intensity distribution with a minimum power fluctuation and therefore an optimized power budget. For this purpose, an objective function¹⁰ relating all terms of power fluctuations is generated. By optimizing the objective function, a well balanced fan-out distribution can be reached. For our problem, an obvious objective function is the sum of the square value of the differences between the fan-out intensities and their average. If we define the intensity of the incident signal beam as 1, after taking into account Eqs. (4) and (5), the average fan-out intensity is given by

$$\bar{P}=\frac{1}{2N-3}. \quad (9)$$

The objective function is then expressed as

$$E = E_1 + E_2 \tag{10}$$

where

$$E_1 = \sum_{i=1}^M \left[\sum_{\substack{j=1 \\ j \neq i}}^N W_{1ij} \left(\frac{P_{ij}}{\bar{P}} - 1 \right)^2 + \sum_{j=2}^{N-1} W'_{1ij} \left(\frac{P'_{ij}}{\bar{P}} - 1 \right)^2 \right] \tag{11}$$

for P_{ij} and $P'_{ij} \geq \bar{P}$,

$$E_2 = \sum_{i=1}^M \left[\sum_{\substack{j=1 \\ j \neq i}}^N W_{2ij} \left(\frac{\bar{P}}{P_{ij}} - 1 \right)^2 + \sum_{j=2}^{N-1} W'_{2ij} \left(\frac{\bar{P}}{P'_{ij}} - 1 \right)^2 \right] \tag{12}$$

for P_{ij} and $P'_{ij} < \bar{P}$,

where $W_{1ij}^{(r)}$ and $W_{2ij}^{(r)}$ are weight factors, $M = N/2$ when N is an even number, and $M = (N + 1)/2$ when N is an odd number.

An optimized fan-out distribution should result in a minimum value in the objective function E , which implies that the first derivative of E with respect to each η_i ($i = 1, 2, \dots, N-1$) is equal to zero, i.e.,

$$\frac{\partial E}{\partial \eta_i} = 0 \quad i = 2, \dots, N-1. \tag{13}$$

4 Optimization Results and Implications

In accordance with our previous work⁵ we optimize the fan-out distribution for the case in which $N = 9$ (see Fig. 3). A computer program was employed to provide the fan-out intensities and other related parameters. The seven non-linear equations [Eq. (13)] with $i = 2, 3, \dots, 8$ are then solved numerically using the Levenberg-Marquardt algorithm¹¹ and a finite-difference approximation to the Jacobian, subject to the constraint of

$$0 < \eta_2, \dots, \eta_8 < 1. \tag{14}$$

The statistical weight we used in our calculation has the exponential form, i.e.,

$$W_{1ij}^{(r)} = \exp \left[A \left(\frac{P_{ij}}{\bar{P}} - 1 \right) \right] \quad \text{for } P_{ij}^{(r)} \geq \bar{P}, \tag{15}$$

$$W_{2ij}^{(r)} = \exp \left[B \left(\frac{\bar{P}}{P_{ij}} - 1 \right) \right] \quad \text{for } P_{ij}^{(r)} < \bar{P}, \tag{16}$$

where the superscript (r) means either with or without the prime for the case we are dealing with. The change of the statistical weight is carried out by increasing the A and B values. Figure 4 is the plot of the variation of the ratio of the maximum and minimum fan-out intensities as a function of A and B . These maximum and minimum values are obtained by comparing the optimized P_{ij} 's ($i = 1, \dots, 5, j = 1, \dots, 9, i \neq j$) and P'_{ij} 's ($i = 1, \dots, 5, j = 2, \dots, 8$) under a selected pair of A and B . The optimized fan-out distribution can be located by finding the minimum ratio. Figure 5 shows the equal topological lines of Fig. 4. From

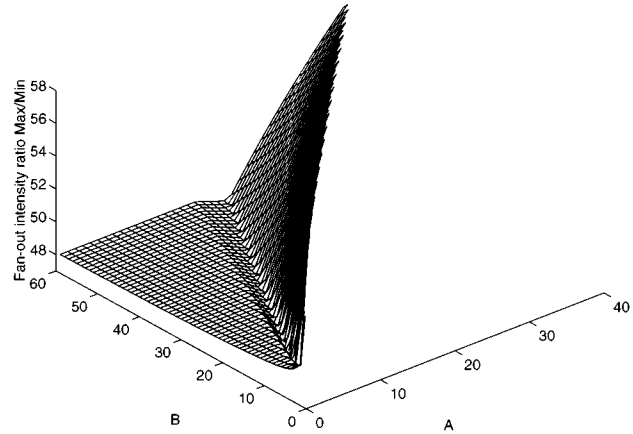


Fig. 4 Ratio between the maximum and minimum fan-out intensities among 240 (16×15) beams as a function of coefficients A and B .

this figure and our calculation result, it is clear that this minimum ratio is 47.5, and this occurs only after A reaches 6.0 and B reaches 16.0. For calculation of the optimized diffraction distribution, we took A and B up to 22 and 58, respectively. The optimized diffraction efficiency distribution is determined to be

$$(\eta_1, \eta_2, \dots, \eta_9) = (1.0, 0.3757, 0.2303, 0.1671, 0.1274, 0.1298, 0.2024, 0.4451, 0.0), \tag{17}$$

and the optimized fan-out intensities are given in Table 1. The average value of the fan-out [from Eq. (9)] intensities is 0.06667. This diffraction efficiency distribution represents the optimized power fluctuation among 240 (16×15) interconnects.

To verify the validity of our calculation, we further developed another objective function, which has the arithmetic form of

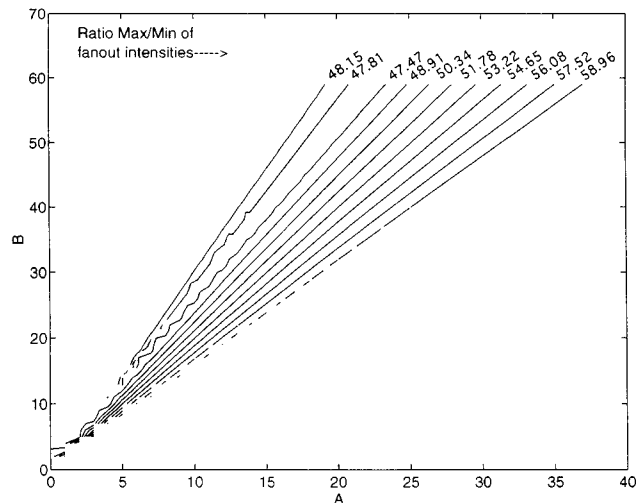


Fig. 5 Equal topologies of Fig. 4.

Table 1 Optimized fanout distribution from our calculation.

Fan-out \ j	1	2	3	4	5	6	7	8	9
P_{ij}	0	0.27791	0.05833	0.02493	0.01860	0.01852	0.01698	0.01587	0.02131
P'_{ij}	0	0.16213	0.05758	0.02972	0.01653	0.01587	0.01587	0.01586	0
P_{2j}	0.44513	0	0.05853	0.02502	0.01867	0.01859	0.01703	0.01591	0.02138
P'_{2j}	0	0.17921	0.05777	0.02982	0.01659	0.01591	0.01591	0.01590	0
P_{3j}	0.07579	0.04219	0	0.02490	0.01858	0.01850	0.01696	0.01569	0.02129
P'_{3j}	0	0.04218	0.56723	0.02968	0.01651	0.01586	0.01586	0.01569	0
P_{4j}	0.02993	0.01666	0.02384	0	0.01858	0.01850	0.01696	0.01569	0.02128
P'_{4j}	0	0.01666	0.01667	0.70316	0.01651	0.01586	0.01586	0.01569	0
P_{5j}	0.02132	0.01587	0.01698	0.01853	0	0.01853	0.01698	0.01587	0.02132
P'_{5j}	0	0.01587	0.01588	0.01588	0.74511	0.01588	0.01588	0.01587	0

$$W_{1ij}^{(r)} = \left(\frac{P_{ij}^{(r)}}{\bar{P}} - 1 \right)^C \quad \text{for } P_{ij}^{(r)} \geq \bar{P}, \quad (18)$$

and

$$W_{2ij}^{(r)} = \left(\frac{\bar{P}}{P_{ij}^{(r)}} - 1 \right)^D \quad \text{for } P_{ij}^{(r)} < \bar{P}. \quad (19)$$

The corresponding fan-out intensity ratio diagram (Max/Min) is shown in Fig. 6. Because of the rapid ascending characteristic of the exponential function, we expect that the number of iterations in this calculation should be much larger in getting to the optimized result than the first approach. This is verified by viewing Fig. 6. In this figure, we calculated for the case of C from 100 to 160 and D from 200 to 280. Comparison shows that this iteration reaches our same optimization condition, i.e., a maximum-to-minimum fan-out ratio of 47.47, after $C = 125$ and $D = 217$, which is derived from Fig. 7.

To compare with the scenario in which all the multiplexed holograms have the same diffraction efficiency, we show in Fig. 8 the variation between the defined Max/Min with the diffraction efficiencies. The range for the value of the diffraction efficiencies are from $>1\%$ to $<50\%$. An

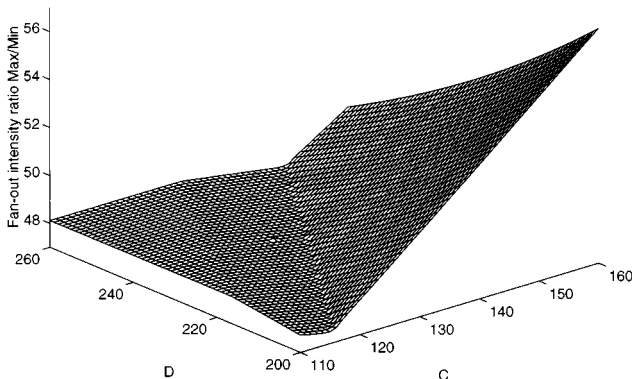


Fig. 6 Same as Fig. 5, but using the statistical weight of arithmetic power form for the objective function.

inspection of Fig. 8 gives a minimum Max/Min power ratio of ≈ 250 , which is much larger than the optimized result presented.

In the proposed bidirectional optical bus architecture, affiliated with each board there is an optoelectronic transceiver that contains a laser diode to provide the input signal for the backplane bus and a photodiode to receive the surface-normal fan-out signal from the backplane bus. The sensitivity of a photodiode is a function of laser power, modulation speed, bit error rate and the wavelength of the signal carrier. For a $p-i-n$ field-effect transistor (FET) photodiode with a quantum efficiency of 50% at $1.3 \mu\text{m}$, if the data transfer rate is 1.2 Gbit/s, and the required error probability after amplification of the detector signal is less than 10^{-15} , then the minimum modulated power required at the detector site is¹² about 1.0×10^{-4} W. Because the minimum fan-out intensity we derived out of our calculation is 1.57% of the input, the minimum input power required is determined to be 7.0 mW. This result considers the fanouts from two surface-normal directions illustrated in Fig. 3, where 16 $[9 + (9-2)]$ fanouts instead of 9 are provided as the case in Ref. 5. Experimental demonstration without fan-

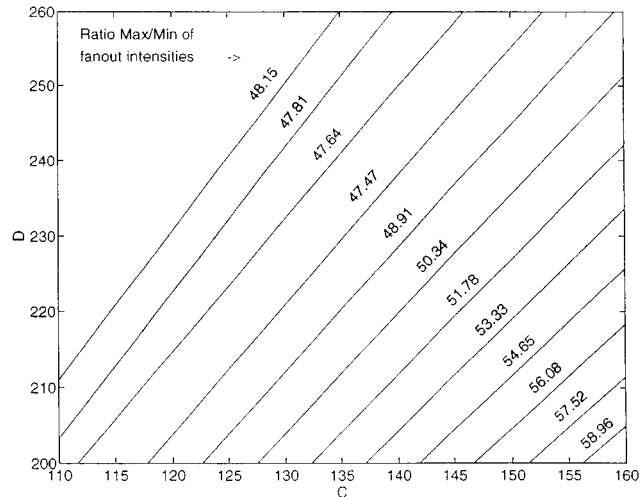


Fig. 7 Equal topologies of Fig. 6.

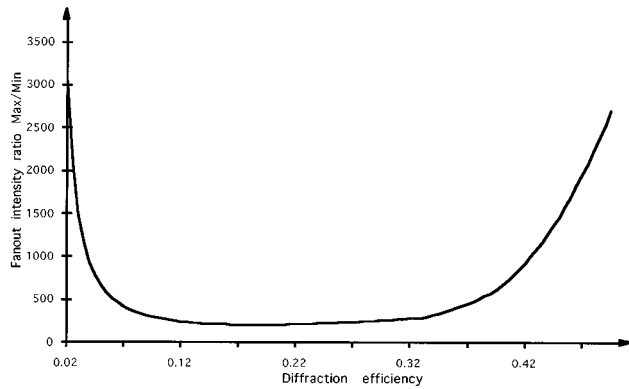


Fig. 8 Variation of the ratio between the maximum and minimum fan-out intensities among 240 (16×15) beams with diffraction efficiencies of the multiplexed holograms (with all the multiplexed holograms having the same diffraction efficiency).

out intensity optimization can be found in Ref. 5. We are working on the prototype of an optimized optical backplane bus based on the theoretical investigation presented herein. Further results will be presented in a separate publication.

5 Conclusions

In summary, we present the theory of optimization of fan-out intensity distribution of the bidirectional optical backplane bus, aimed at balancing the fan-out intensities among different channels using an objective function. Employment of two different statistical weights in the objective function leads to the same optimized result. For a bidirectional optical bus with 9 boards on one side, the optimization result shows that the minimum fan-out intensity is 1.5% of the incident power, under which the minimum laser diode power is 7.0 mW for a system with a speed of 1.2 Gbit/s and a bit error rate of 10^{-15} operating at $1.3 \mu\text{m}$. Based on the phase-matching condition, the surface-normal fan-out beams come out of both directions. Therefore, the best hardware implementation scheme integrates the processor/memory boards in both sides of the backplane bus. As a result, the optimal number of the processor/memory boards shall be 16, i.e., $9 + (9 - 2)$, rather than 9, when both sides of the backplane are employed.

References

1. P. Sweazey, "Limits on performance of backplane buses," in *Digital Bus Handbook*, J. DeGiacomo, Ed., McGraw-Hill, New York (1990).
2. J. W. Goodman, F. J. Leonberger, S. Y. Kung and R. A. Athale, "Optical interconnects for VLSI systems," *Proc. IEEE* **72**, 850–866 (1984).
3. A. Husain, T. Lane, C. Sullivan, J. Bristow and A. Guha, "Optical backplanes for massively parallel processors and demonstration in the connection machine," presented at Government Microcircuit Application Conf., Nov. 1990, Las Vegas, NV, Palisades Institute for Research.
4. R. T. Chen, "VME optical backplane bus for high performance computer," *Optoelectron. Device Technol.* **9**, 81–94 (1994).
5. S. Natarajan, C. Zhao and R. T. Chen, "Bi-directional optical backplane bus for general-purpose multi-processor board-to-board optoelectronic interconnects," *J. Lightwave Technol.* **13**, 1031–1040 (1995).
6. H. P. Herzig and R. Dandliker, "Diffractive components: holographic optical elements," in *Perspectives for Parallel Optical Interconnects*, P. Lalanne and P. Chavel, Eds., Springer-Verlag, New York (1993).
7. T. K. Gaylord and M. G. Moharam, "Analysis and applications of optical diffraction by gratings," *Proc. IEEE* **73**, 894–937 (1985).
8. S. K. Case, "Coupled-wave theory for multiply exposed thick holographic gratings," *J. Opt. Soc. Am.* **65**, 724–729 (1975).
9. R. Kowarschik, "Diffraction efficiency of sequentially stored gratings in transmission volume holograms," *Opt. Acta* **25**, 67–81 (1978).
10. E. Pinney and D. B. McWilliams, *Management Science: An Introduction to Quantitative Analysis for Management*, Harper & Row Publishers, New York (1982).
11. J. More, B. Garbow and K. Hillstrom, *User Guide for MINPACK-1*, Argonne National Labs Report ANL-80-74, Argonne, IL (1980).
12. A. Yariv, *Introduction to Optical Electronics*, 2nd ed., McGraw-Hill, New York (1976).

Chunhe Zhao is a graduate student in the Department of Electrical and Computer Engineering of the University of Texas at Austin. His interests include optical and optoelectronic interconnection, optical neural network, very large scale integration related design and fabrication processes. Now he is working on his PhD. He is a student member of SPIE.

Ray T. Chen is currently a faculty member of the Microelectronics Research Center at the University of Texas, Austin. He was with Physical Optics Corporation, Torrance, California, from June 1988 to August 1992. He has been a principal investigator for over 40 awarded research proposals sponsored by many subdivisions of the Department of Defense, the National Science Foundation, the Department of Energy, the National Aeronautics and Space Administration and private industries such as Cray Research, GE, Honeywell, Boeing, Radiant Research, Physical Optics Corporation and Novex Corp. His research topics cover 2-D and 3-D optical interconnections, polymer-based integrated optics, polymer waveguide amplifier, graded-index polymer waveguide lens, active optical backplane, traveling wave electro-optic polymer waveguide modulator, GaAs all-optical cross bar switch, holographic lithography and holographic optical elements. He has served as the chairman and a program committee member for over 20 domestic and international conferences organized by SPIE, IEEE and PSC. He is also an invited lecturer for the short course of optical interconnects for the international technical meetings organized by SPIE. Dr. Chen has over 150 publications including over 25 invited papers. He has served as a consultant for various federal government agencies and private companies and delivered numerous invited talks in the professional societies. Dr. Chen is an active member of IEEE, LEOS, SPIE, OSA and PSC.